Published in final edited form as:
Cell Rep. 2014 February 13; 6(3): 445–454. doi:10.1016/j.celrep.2014.01.002.

Recycling endosome tubule morphogenesis from sorting endosomes requires the kinesin motor KIF13A

Cédric Delevoye[1,2,*], **Stéphanie Miserey-Lenkei**[1,3,#], **Guillaume Montagnac**[1,4,#], **Floriane Gilles-Marsens**[1,2], **Perrine Paul-Gilloteaux**[1,5], **Francesca Giordano**[1,2,7], **François Waharte**[1,5], **Michael S. Marks**[6], **Bruno Goud**[1,3], and **Graça Raposo**[1,2,5]

[1]Institut Curie, Centre de Recherche, Paris, F-75248 France

[2]Structure and Membrane Compartments CNRS UMR144, Paris, F-75248 France

[3]Molecular Mechanisms of Intracellular Transport CNRS UMR144, Paris, F-75248 France

[4]Membrane and Cytoskeleton Dynamics CNRS UMR144, Paris, F-75248 France

[5]Cell and Tissue Imaging Facility (PICT-IBiSA) CNRS UMR144, Paris, F-75248

[6]Department of Pathology & Laboratory Medicine, Children's Hospital of Philadelphia and University of Pennsylvania, Philadelphia, PA 19104 USA

Summary

Early endosomes consist of vacuolar sorting and tubular recycling domains that segregate components fated for degradation in lysosomes or reuse by recycling to the plasma membrane or Golgi. The tubular transport intermediates that constitute recycling endosomes function in cell polarity, migration and cytokinesis. Endosomal tubulation and fission require both actin and intact microtubules, but while factors that stabilize recycling endosomal tubules have been identified, those required for tubule generation from vacuolar sorting endosomes remain unknown. We show that the microtubule motor KIF13A associates with recycling endosome tubules and controls their morphogenesis. Interfering with KIF13A function impairs the formation of endosomal tubules from sorting endosomes with consequent defects in endosome homeostasis and cargo recycling. Moreover, KIF13A interacts and cooperates with RAB11 to generate endosomal tubules. Our data illustrate how a microtubule motor couples early endosome morphogenesis to its motility and function.

Keywords

Kinesin; microtubule; tubule formation; endosomal sorting and recycling

[*]Corresponding author: Cédric Delevoye, Institut Curie, CNRS-UMR144, 26 Rue d'Ulm, 75248 Paris cedex, Tel: +33156246583 Fax: +33156246421 cedric.delevoye@curie.fr.
[7]Present address: Membrane Dynamics and Intracellular Trafficking, Institut Jacques Monod, UMR 7592, CNRS, Université Paris Diderot, Sorbonne Paris Cité, F-75013 Paris, France.
[#]Both authors contributed equally to the work.

The authors declare no conflict of interests.

Introduction

Recycling endosomes (RE) constitute a network of tubular membranes that function to facilitate homeostatic maintenance of plasma membrane receptors in metazoan cells. Internalized cargoes such as transferrin receptor (TfR) are diverted within sorting endosomes (SE) into tubules destined for the plasma membrane, thereby avoiding lysosomal degradation (Maxfield and McGraw, 2004). RE tubules, which form as SE vacuoles mature into multivesicular endosomes (MVEs), promote sorting and trafficking of components not only to the cell surface but also to the trans-Golgi network (TGN), lysosomes and related organelles (Grant and Donaldson, 2009; Marks et al., 2013). RE-dependent transport regulates such diverse cellular functions as cell polarity, migration and cytokinesis (Grant and Donaldson, 2009).

Depending on the cell type, RE tubules distribute either in the pericentriolar region where they define the endosomal recycling compartment (ERC) (Yamashiro et al., 1984), or more peripherally without forming a distinguishable ERC (e.g. in melanocytes, (Delevoye et al., 2009)). RE motility requires actin and microtubules (Grant and Donaldson, 2009). Whereas actin-based myosin motors generally support short-range movements and membrane tension (Loubery and Coudrier, 2008), microtubule-associated motors drive long-range trafficking of organelles and protein cargoes. Whereas the dynein-dynactin complex drives cargoes toward the cell center (Allan, 2011), kinesin superfamily proteins (KIFs) mediate cargo motility mainly towards microtubule plus-ends from the microtubule-organizing center to the cell periphery, linking cargo sorting to carrier transport (Hirokawa et al., 2009).

Microtubule motor activity is required for organelle positioning and morphogenesis. *In vitro*, KIFs generate the driving force for membrane tubulation and fission required for cargo trafficking (Roux et al., 2002), but only KIF5B has been shown *in vivo* to form TGN-derived tubular carriers (Kreitzer et al., 2000). At early endosomes, the kinesin-3 KIF16B regulates the motility of SE (Hoepfner et al., 2005) or common RE in epithelial cells (Perez Bay et al., 2013), and the kinesin-2 KIF3B has been implicated in the endosomal sorting of Tf (Schonteich et al., 2008). Although RE tubules align along microtubules near SE (Willingham et al., 1984), the KIF required for generation of RE tubules from the vacuolar SE has not been defined.

The plus-end directed kinesin-3, KIF13A, is a good candidate to fulfill such a function. In pigment cells, KIF13A coordinates the positioning of RAB11-positive endosomes in the cell periphery with protein sorting to nearby melanosomes (Delevoye et al., 2009). Here we demonstrate that KIF13A dynamically associates with RE and is essential for the generation of RE tubules from SE and for their distribution toward the cell periphery. Moreover, KIF13A binds to the active GTP-bound form of the RE-associated RAB11 to control endosomal sorting and recycling of an endosomal cargo.

Results and Discussion

KIF13A associates with Recycling Endosomes

We first investigated KIF13A localization in HeLa cells by immunofluorescence microscopy (IFM). A KIF13A-YFP fusion protein localized to clustered puncta at the cell periphery that co-distributed partially with classical RE components, as shown by Mander's coefficient (MC) analysis of overlap with internalized transferrin (Tf) (0.43±0.1; $p<0.001$), RAB11A (0.23±0.04; $p<0.05$) (Figures 1A–1B, arrows), Tf Receptor (TfR) (0.43±0.04; $p<0.01$), RCP (Rab coupling protein or RAB11 FIP1) (0.57±0.2; $p<0.05$), and the γ-adaptin subunit of the adaptor AP-1 (0.66±0.2; $p<0.05$) (Figures S1A–S1C, arrows) as previously described (Delevoye et al., 2009; Nakagawa et al., 2000). KIF13A did not co-localize with

markers of the SE (EEA1; 0.02±0.02) or late endosomes/lysosomes (LAMP1; 0.03±0.02) (Figures S1D–S1E). Although KIF13A was proposed to mobilize carrier vesicles from the TGN (Nakagawa et al., 2000), KIF13A did not colocalize with TGN46 (0.004±0.005) and KIF13A overexpression did not alter TGN46 distribution (Figure S1F). These observations support our previous studies showing that endogenous KIF13A localized partially with RE markers in melanocytes (Delevoye et al., 2009) and show that the bulk of KIF13A associates with RE.

KIF13A generates endosomal tubules in a microtubule- and motor-dependent manner

Expression of KIF13A-YFP (Figures 1A and S1A, arrows; and Movie 1), but not of GFP alone (Figure S2A) caused a pool of Tf/TfR-positive endosomes to accumulate at the cell periphery. Moreover, over-expression of KIF13A – but not GFP – induced dramatic tubulation of membranes that labeled for endogenous RAB11A and RCP (Figures 1B, S1B, arrows, Figure S2B and Movie 2). KIF13A-positive tubular membranes aligned along microtubules (Figure S2C, arrows). Disruption of the microtubule network by treatment with nocodazole (NZ) prevented the formation of KIF13A-induced RE-tubules (Figures 1C–1D and S2D), as compared to DMSO-treated controls (Figures S2E–S2F), without altering the endosomal localization of KIF13A (Figure 1D, arrows). These data indicate that KIF13A drives the formation of RE-tubules toward the plus-end of microtubules, ferrying RE cargoes toward the cell periphery.

To investigate whether KIF13A-dependent RE-tubulation requires its motor activity, we expressed GFP-tagged KIF13A-ST containing the KIF13A stalk (S) (residues 351–1306) and tail (T) (1307–1770) domains but lacking the motor domain. Strikingly, KIF13A-ST localized to vesicular structures devoid of tubules in which internalized Tf (0.13±0.06; $p<0.05$), RAB11A (0.10±0.02, $p<0.05$), TfR (0.15±0.09; $p<0.05$) and AP-1 (0.65±0.04; $p<0.05$) partially co-distributed (Figures 1E–1F and S3A–S3B, arrows) but not LAMP1 (0.08±0.07) or TGN46 (0.001±0.002) (Figures S3C–S3D). These findings reveal that the KIF13A motor domain is required to generate tubular intermediates and the stalk and/or tail confers early endosomal localization.

KIF13A initiates endosomal tubulation at sorting endosomes

Vacuolar SE maturation is tightly associated with the formation, extension and fission of RE tubules (Mesaki et al., 2011). If KIF13A were necessary for RE tubulation, we would predict that KIF13A depletion should impair: (1) the generation of RE tubules from vacuolar SE; (2) the sorting of cargo, such as Tf, into recycling tubular intermediates; and (3) the positioning of RE-positive carriers away from SE. Our data support this prediction. First, KIF13A siRNA-treated cells (Figure 2A) accumulated enlarged Tf-positive endosomal structures that were closely apposed to EEA1-positive early endosomes and that contained the Mannose-6-Phosphate receptor (M6PR) as cargo (which cycles between endosomes and TGN; Figures 2B and S4A, respectively), but not TGN or late endosome components (TGN46 and CD63, respectively) (Figures S4A–S4B). Second, we analyzed by electron microscopy (EM) control- and KIF13A-depleted cells that had internalized Tf conjugated to horseradish peroxidase (Tf-HRP). The percentage of Tf-HRP-containing tubules (identified by the electron dense DAB reaction product) was consistently decreased in KIF13A-depleted cells as compared to control (43±2% and 60±2%; $p<0.001$; respectively) (Figure 2C, arrows; and see below). Third, RAB11-positive structures were observed in close apposition to these enlarged Tf-positive endosomes (Figure S4C, arrowheads) suggesting that RE motility away from the SE is impaired (see below). Together, these data suggest that KIF13A is required to generate RE tubules from the vacuolar SE.

A fourth prediction of our hypothesis is that KIF13A should first be recruited to vacuolar SE that harbor EEA1, but that rapid motility would prevent its accumulation at the site of recruitment. Therefore, to detect association with the donor compartment, we examined the distribution of the motorless KIF13A-ST. Unlike full-length KIF13A (Figure S1D; 0.02±0.02), KIF13A-ST overlapped extensively (5-fold higher) with EEA1 (Figure S3E, arrows; 0.11±0.04; $p<0.05$). KIF13A-ST also co-distributed with EEA1-positive endosomes in MEF cells derived from *Kif13a*$^{-/-}$ mice (Zhou et al., 2013) (Figure S3F). Together, our data indicate that KIF13A binds to EEA1-positive vacuolar SE via its stalk and/or tail domains and drives the generation of RE tubules along microtubule tracks.

KIF13A modulates the sorting of recycling cargoes within endosomal tubular intermediates

Recycling endosomes facilitate transport of a cohort of TfRs and associated Tf to the cell surface after internalization, whereas a larger proportion is recycled directly from SE (Sheff et al., 1999; van der Sluijs et al., 1992). Consistent with a role for KIF13A specifically in RE function, Tf recycling was decreased by 15% in KIF13A-inactivated cells relative to controls (Figure 2E) – consistent with the ≤20% decrease observed upon disruption of RAB11 or RCP function (Peden et al., 2004; Ullrich et al., 1996) – without any noticeable change in Tf uptake (C.D., unpublished data). The inhibition of Tf recycling by KIF13A depletion was observed by 6 min of chase (Figure 2E), when Tf- HRP begins to appear in vacuolar endosome-associated tubular membranes (Willingham et al., 1984), suggesting that KIF13A functions at an early step in recycling cargo segregation. Consistent with a requirement for KIF13A in recycling of endosomal cargoes to the cell surface, quantification on live cells using TIRF microscopy indicated that the number of mobile Tf-positive vesicles underneath the plasma membrane was reduced by 78±6.4 % in KIF13A-depleted cells relative to controls (Figure 2F; $p<0.005$).

We used EM and DAB histochemistry to identify the endosomal structures in which the remaining Tf-HRP accumulates upon KIF13A depletion. As described (Willingham et al., 1984; Yamashiro et al., 1984), control cells harbored electron dense tubules characteristic of RE (Figure 2C, arrows). KIF13A-depleted cells not only lacked such tubules (see above), but strikingly concentrated Tf-HRP in organelles with morphological features of MVEs (Figure 2C, arrowheads and quantitated in Figure 2D,). To determine if these MVEs were classical late endosomes destined to fuse with lysosomes, we compared the fate of internalized Tf and EGF (Epidermal Growth Factor) in control- and KIF13A-depleted cells. After 30 min of chase, Tf- and EGF-positive endosomes were segregated and concentrated in the center of control cells (Figure 2B; arrowheads). In KIF13A-depleted cells, internalized Tf and EGF still labeled distinct endosomal populations (Figure 2B, arrowheads). However, Tf localized to dispersed and enlarged compartments in the vicinity of EEA1-positive endosomes that were distinct from late endosomes (Figures 2B and S4B), whereas EGF co-distributed with CD63 in late endosomes (Figure S4B, arrows). These observations indicate that Tf is not missorted to conventional degradative MVEs in the absence of KIF13A. Consistently, whereas EGFR was degraded at similar rates in control- and KIF13A-depleted cells, TfR was not degraded to a significant extent in either cell population (Figure 2G). Thus, although the compartments that accumulate Tf upon KIF13A depletion morphologically resemble small MVEs, they represent abnormal early endosomes that are unable to tubulate. Our data are consistent with the accumulation of Tf-positive MVE-like organelles without impaired degradative MVE biogenesis upon inhibition of early endosomal recycling (Bright et al., 2001).

To further support these results, we assessed internalized Tf localization in *Kif13a*$^{-/-}$ MEFs. IFM analyses revealed that more than half of these cells harbored enlarged EEA1-positive

endosomes that contained internalized Tf (51±0.3%) and accumulated M6PR (51±6%) (Figure S4E) whereas control cells did not (C.D., unpublished data). Enlarged vacuolar structures containing few or no internal membranes were also observed by conventional EM (Figure S4F, arrows). These results indicate that KIF13A-dependent recycling tubule formation is required for normal endosomal morphology and homeostasis. Together, our data support the conclusion that KIF13A generates recycling endosomal tubular intermediates from vacuolar SE, favoring Tf sorting into tubular RE carriers destined for the plasma membrane.

KIF13A pulls RAB11-positive endosome tubules

We next investigated in live cells the dynamic behavior of KIF13A relative to a RE-associated protein, RAB11A. KIF13A-YFP localized to dynamic tubular structures that accumulated at the cell periphery together with Tf and RAB11A (Figure S4D and Movies 1–2). KIF13A itself accumulated at the cell periphery, as 87±16% of KIF13A labeling distributed within the nearest 30% of the cell radius to the cell edge. In cells co-expressing KIF13A-YFP and mCherry-RAB11A, KIF13A localized to and induced the formation of highly dynamic RAB11-positive tubules that extended towards the cell periphery (Figure 3A and Movie 2). Both proteins were distributed all along the tubules (0.75±0.1; $p<0.001$) as also observed on fixed cells (Figure 1B). By contrast, coexpressed RAB4A was excluded from the majority of KIF13A-containing tubules (Movie 4; 0.08±0.05; p<0,001). Furthermore KIF13A was most enriched at the tips of the tubules (Figure 3A, arrows and Movie 2), consistent with the accumulation of kinesins at the tips of membrane tubes *in vitro* (Roux et al., 2002). By contrast, the motorless KIF13A-ST co-distributed with RAB11A in large vesicular structures devoid of emanating tubules (Movie 3).

To further support these results, we assessed the distribution of mCherry-RAB11A in *Kif13a*$^{-/-}$ MEFs co-transfected with KIF13A or with GFP or the motorless KIF13A-ST as controls. In *Kif13a*$^{-/-}$ MEFs co-expressing RAB11A with GFP or KIF13A-ST, RAB11A was mainly distributed in vesicles closely apposed to the nucleus (Figure 3B), suggesting predominant minus end-directed microtubule transport; RAB11A accumulated in the cell periphery in only 10% of cells co-expressing either GFP or KIF13A-ST (Figure 3B; 9±1% and 11±0.6%, respectively). By contrast, RAB11A distributed toward the periphery of cells co-expressing full-length KIF13A (Figure 3B; 49±0.8%; $p<0.001$). As in HeLa cells, RAB11A co-distributed partially with co-expressed KIF13A or KIF13A-ST in *Kif13a*$^{-/-}$ MEFs (Figure 3B). These data support the conclusion that intact KIF13A drives the transport of RAB11-positive endosomal structures towards the plasma membrane.

Together, our data show that KIF13A pulls tubules from SE specifically within the RAB11-dependent recycling pathway. Endosomal tubules are stabilized by proteins such as EHD (Eps15 homology domain-containing proteins) or BAR domain-containing proteins (such as sorting nexins) that sense curved membranes (Naslavsky and Caplan, 2011; van Weering et al., 2010), but whether these proteins impose membrane curvature has remained controversial. We propose that KIF13A functions upstream of these machineries to generate the tubules that are then stabilized by curvature sensing proteins.

KIF13A interacts with the active form of RAB11

KIF13A depletion phenocopies impaired RAB11 function in causing Tf to accumulate within MVEs and reducing Tf recycling (Ullrich et al., 1996). We thus next tested whether KIF13A and RAB11 function together. As other Rab GTPases bind to microtubule motors (Horgan and McCaffrey, 2011) and KIF13A-ST localizes to early endosomes (Figures 1E–F and S3A–B and E), we first tested whether KIF13A interacts with RAB11 by a yeast two-hybrid assay (Y2H) using the S and/ or T domains of human KIF13A (Delevoye et al., 2009;

Nakagawa et al., 2000) (Figure 3C) as baits. Interactions were found with activated forms of RAB11A and RAB11B (Q/L mutants) and wild-type RAB25 (Figure 3D), a RAB11 family member with an endogenous amino acid substitution (Q71L) that mimics a dominant active mutation (Goldenring et al., 1993). By contrast, KIF13A domains did not interact with any of the constitutively inactive RAB11 mutants (S or T/N mutations), or with the active forms of RAB1A, RAB6A or RAB27A (Figure 3D). The Y2H results were confirmed by GST pull-down assays in which endogenous KIF13A was pulled down by GST-RAB11A loaded with GTPγS, but not with GDP, and not by RAB6A or RAB4A as controls (Figure 3E; black stars). Moreover, Flag-tagged RAB11A co-immunoprecipitated with KIF13A, KIF13A-ST and KIF13A-T (Figure 3F). Finally, *in vivo* interactions between RAB11A and KIF13A were confirmed by Forster Resonance Energy Transfer (FRET)/Fluorescence Lifetime Imaging (FLIM) experiments in live HeLa and melanocytic MNT-1 cells (Figures 3G–3H and C.D., unpublished data). A decrease in the mean YFP fluorescence lifetime showed statistically significant FRET between KIF13A and RAB11A in both cell lines as compared to cells that only expressed KIF13A (Figures 3G–3H; 2.45±0.27ns and 2.51±0.15ns; $p<0.05$, respectively). As an additional control, no FRET was detected in HeLa cells co-expressing KIF13A-YFP and RAB30 (Figure 3H), which localizes to Golgi membranes and to a subset of RAB11-positive endosomes (Kelly et al., 2012; Thomas et al., 2009). Interestingly, FRET between RAB11 and KIF13A was higher in MNT-1 cells (Figure 3H; 2.19±0.42ns as compared to 2.53±0.31ns in control; $p<0.001$,) in which KIF13A controls endosomal positioning required for cargo sorting to maturing melanosomes (Delevoye et al., 2009). Together, our results show that KIF13A binds to the active form of RAB11 via at least two binding sites in the stalk and tail regions. The results of FLIM/FRET and Y2H analyses suggest that the interaction between KIF13A and RAB11 is direct, but we cannot exclude the existence of an intermediate binding partner *in vivo*.

RAB11 and KIF13A cooperate to generate recycling endosomal tubules

The binding of KIF13A to all members of the RAB11 family (Figure 3D) suggests that KIF13A operates from several RE subdomains. To test whether RAB11 cooperates with KIF13A to generate RE tubules from SE, we analyzed the ability of RAB11-depleted cells to form KIF13A-positive RE tubules. Although KIF13A interacts strongly with RAB25 (Figure 3D) and RAB25 is expressed in HeLa cells, RAB25 depletion did not impair KIF13A-dependent Tf tubulation or peripheralization (C.D., unpublished data), indicating that RAB25 alone is not required for KIF13A function. However, when cells were depleted of all three RAB11 isoforms – RAB11A, B and RAB25 – we observed an over 3-fold increase in the percentage of cells that were unable to generate KIF13A-positive RE tubules as compared to controls (Figure 4A, white star; $p<0.001$). Instead, RAB11-depleted cells accumulated enlarged KIF13A- and Tf-positive punctate structures (Figure 4A, arrows). Similar Tf-positive structures were observed in KIF13A non-transfected cells (Figure 4B), indicating that they resulted from RAB11 depletion and not from KIF13A overexpression. These enlarged endosomal structures resembled those observed in KIF13A-depleted cells (Figures 2B and S4A–S4C) since they contained internalized Tf and were apposed to EEA1-positive endosomes (Figure 4B, arrows). These data suggest that KIF13A and RAB11 cooperate at the SE to generate RE tubules.

In this study, we have identified KIF13A as a RE-associated kinesin required for RE tubule morphogenesis. We propose a model (Figure 4C) in which KIF13A at the SE initiates the formation of endosomal tubules along microtubules through its motor activity. The interaction of KIF13A with RAB11 likely occurs at a specific SE subdomain from which both proteins cooperate to extract RE tubule intermediates. Tf is sorted into these intermediates for recycling to the plasma membrane (Figure 4C). As compared to other endosomal kinesins (KIF16B, KIF3B) that control the transport of endosomal carriers

(Hoepfner et al., 2005; Perez Bay et al., 2013; Schonteich et al., 2008), KIF13A couples the trafficking of transport intermediates and their cargoes to organelle morphogenesis. Our model might explain earlier findings showing that KIF13A regulates M6PR distribution to the periphery (Nakagawa et al., 2000), since M6PR cycles through RE after its sorting at the TGN (Ghosh et al., 2003). Likewise a cytokinesis defect observed in KIF13A-depleted cells (Sagona et al., 2010) could reflect impaired targeting of RAB11-positive endosomal tubules to the midbody (Simon and Prekeris, 2008).

Recycling is particularly critical in neurons. Our observations of defective early endosome dynamics in *Kif13a*$^{-/-}$ mice likely explains the defect in anxiety control in these mice, which likely reflects the mistrafficking of specific neuronal receptors (Zhou et al., 2013). Huntington, Alzheimer and Prion diseases are also associated with improper function of RE and associated proteins such as RAB11 (Li and Difiglia, 2011). Analyses of KIF13A function in neuronal subsets might thus lead to new insights into neurological disorders.

Experimental Procedures

Detailed procedures and reagent information are in the Supplemental Experimental Procedures. Mander's coefficients were computed for all stacks of the 3D deconvolved IFM images and the first 20 frames of live cell movies, using WCIF ImageJ. Spatio-temporal gradient of the sequences using G'MIC software (http://gmic.sourceforge.net/) was used to measure the number of mobile particles on live cell TIRF imaging. Unless otherwise specified, all statistical tests were t-test performed using Matlab after testing the normality of the studied distributions by Jarque Bera test.

Supplementary Material

Refer to Web version on PubMed Central for supplementary material.

Acknowledgments

We are grateful to Dr. N. Hirokawa (University of Tokyo, Japan) and Dr. P. van der Sluijs (UMC-U, Utrecht, Netherlands) for generous gifts of reagents; members of the Structure and Membrane Compartment group for critical reading of the manuscript; Dr. J. Boulanger, L. Sengmanivong and V. Fraisier (Spatio Temporal Modeling Imaging and Cellular Dynamics group). The authors greatly acknowledge the Nikon Imaging Centre @ Institut Curie-CNRS. This work was supported by CNRS, INSERM, Institut Curie and Canceropole Ile de France (to GR), National Institutes of Health (NIH) Grant R01 EY015625 from the National Eye Institute (to MSM), Agence Nationale pour la Recherche (ANR 2010 BLAN 121201) and Fondation ARC pour la recherche sur le cancer (ARC grant SL220100601359 to GR and ARC grant 1095 to SML).

References

Allan VJ. Cytoplasmic dynein. Biochem Soc Trans. 2011; 39:1169–1178. [PubMed: 21936784]

Bright NA, Lindsay MR, Stewart A, Luzio JP. The relationship between lumenal and limiting membranes in swollen late endocytic compartments formed after wortmannin treatment or sucrose accumulation. Traffic. 2001; 2:631–642. [PubMed: 11555417]

Delevoye C, Hurbain I, Tenza D, Sibarita JB, Uzan-Gafsou S, Ohno H, Geerts WJ, Verkleij AJ, Salamero J, Marks MS, et al. AP-1 and KIF13A coordinate endosomal sorting and positioning during melanosome biogenesis. The Journal of cell biology. 2009; 187:247–264. [PubMed: 19841138]

Ghosh P, Dahms NM, Kornfeld S. Mannose 6-phosphate receptors: new twists in the tale. Nature reviews Molecular cell biology. 2003; 4:202–212.

Goldenring JR, Shen KR, Vaughan HD, Modlin IM. Identification of a small GTP-binding protein, Rab25, expressed in the gastrointestinal mucosa, kidney, and lung. The Journal of biological chemistry. 1993; 268:18419–18422. [PubMed: 8360141]

Grant BD, Donaldson JG. Pathways and mechanisms of endocytic recycling. Nature reviews Molecular cell biology. 2009; 10:597–608.

Hirokawa N, Noda Y, Tanaka Y, Niwa S. Kinesin superfamily motor proteins and intracellular transport. Nature reviews Molecular cell biology. 2009; 10:682–696.

Hoepfner S, Severin F, Cabezas A, Habermann B, Runge A, Gillooly D, Stenmark H, Zerial M. Modulation of receptor recycling and degradation by the endosomal kinesin KIF16B. Cell. 2005; 121:437–450. [PubMed: 15882625]

Horgan CP, McCaffrey MW. Rab GTPases and microtubule motors. Biochem Soc Trans. 2011; 39:1202–1206. [PubMed: 21936789]

Kelly EE, Giordano F, Horgan CP, Jollivet F, Raposo G, McCaffrey MW. Rab30 is required for the morphological integrity of the Golgi apparatus. Biology of the cell/under the auspices of the European Cell Biology Organization. 2012; 104:84–101. [PubMed: 22188167]

Kreitzer G, Marmorstein A, Okamoto P, Vallee R, Rodriguez-Boulan E. Kinesin and dynamin are required for post-Golgi transport of a plasma-membrane protein. Nat Cell Biol. 2000; 2:125–127. [PubMed: 10655593]

Li X, Difiglia M. The recycling endosome and its role in neurological disorders. Prog Neurobiol. 2011

Loubery S, Coudrier E. Myosins in the secretory pathway: tethers or transporters? Cell Mol Life Sci. 2008; 65:2790–2800. [PubMed: 18726179]

Marks MS, Heijnen HF, Raposo G. Lysosome-related organelles: unusual compartments become mainstream. Current opinion in cell biology. 2013

Maxfield FR, McGraw TE. Endocytic recycling. Nat Rev Mol Cell Biol. 2004; 5:121–132. [PubMed: 15040445]

Mesaki K, Tanabe K, Obayashi M, Oe N, Takei K. Fission of tubular endosomes triggers endosomal acidification and movement. PLoS One. 2011; 6:e19764. [PubMed: 21572956]

Nakagawa T, Setou M, Seog D, Ogasawara K, Dohmae N, Takio K, Hirokawa N. A novel motor, KIF13A, transports mannose-6-phosphate receptor to plasma membrane through direct interaction with AP-1 complex. Cell. 2000; 103:569–581. [PubMed: 11106728]

Naslavsky N, Caplan S. EHD proteins: key conductors of endocytic transport. Trends Cell Biol. 2011; 21:122–131. [PubMed: 21067929]

Peden AA, Schonteich E, Chun J, Junutula JR, Scheller RH, Prekeris R. The RCP-Rab11 complex regulates endocytic protein sorting. Molecular biology of the cell. 2004; 15:3530–3541. [PubMed: 15181150]

Perez Bay AE, Schreiner R, Mazzoni F, Carvajal-Gonzalez JM, Gravotta D, Perret E, Lehmann Mantaras G, Zhu YS, Rodriguez-Boulan EJ. The kinesin KIF16B mediates apical transcytosis of transferrin receptor in AP-1B-deficient epithelia. Embo J. 2013

Roux A, Cappello G, Cartaud J, Prost J, Goud B, Bassereau P. A minimal system allowing tubulation with molecular motors pulling on giant liposomes. Proc Natl Acad Sci U S A. 2002; 99:5394–5399. [PubMed: 11959994]

Sagona AP, Nezis IP, Pedersen NM, Liestol K, Poulton J, Rusten TE, Skotheim RI, Raiborg C, Stenmark H. PtdIns(3)P controls cytokinesis through KIF13A-mediated recruitment of FYVE-CENT to the midbody. Nat Cell Biol. 2010; 12:362–371. [PubMed: 20208530]

Schonteich E, Wilson GM, Burden J, Hopkins CR, Anderson K, Goldenring JR, Prekeris R. The Rip11/Rab11-FIP5 and kinesin II complex regulates endocytic protein recycling. Journal of cell science. 2008; 121:3824–3833. [PubMed: 18957512]

Sheff DR, Daro EA, Hull M, Mellman I. The receptor recycling pathway contains two distinct populations of early endosomes with different sorting functions. The Journal of cell biology. 1999; 145:123–139. [PubMed: 10189373]

Simon GC, Prekeris R. Mechanisms regulating targeting of recycling endosomes to the cleavage furrow during cytokinesis. Biochem Soc Trans. 2008; 36:391–394. [PubMed: 18481966]

Thomas C, Rousset R, Noselli S. JNK signalling influences intracellular trafficking during Drosophila morphogenesis through regulation of the novel target gene Rab30. Dev Biol. 2009; 331:250–260. [PubMed: 19427848]

Ullrich O, Reinsch S, Urbe S, Zerial M, Parton RG. Rab11 regulates recycling through the pericentriolar recycling endosome. The Journal of cell biology. 1996; 135:913–924. [PubMed: 8922376]

van der Sluijs P, Hull M, Webster P, Male P, Goud B, Mellman I. The small GTP-binding protein rab4 controls an early sorting event on the endocytic pathway. Cell. 1992; 70:729–740. [PubMed: 1516131]

van Weering JR, Verkade P, Cullen PJ. SNX-BAR proteins in phosphoinositide-mediated, tubular-based endosomal sorting. Semin Cell Dev Biol. 2010; 21:371–380. [PubMed: 19914387]

Willingham MC, Hanover JA, Dickson RB, Pastan I. Morphologic characterization of the pathway of transferrin endocytosis and recycling in human KB cells. Proc Natl Acad Sci U S A. 1984; 81:175–179. [PubMed: 6141558]

Yamashiro DJ, Tycko B, Fluss SR, Maxfield FR. Segregation of transferrin to a mildly acidic (pH 6.5) para-Golgi compartment in the recycling pathway. Cell. 1984; 37:789–800. [PubMed: 6204769]

Zhou R, Niwa S, Guillaud L, Tong Y, Hirokawa N. A molecular motor, KIF13A, controls anxiety by transporting the serotonin type 1A receptor. Cell Rep. 2013; 3:509–519. [PubMed: 23438369]

Highlights

- The kinesin-3 KIF13A associates with endosomal tubules
- KIF13A controls the morphogenesis of recycling tubules from sorting endosomes
- KIF13A interacts with the GTP-bound form of RAB11
- KIF13A and RAB11 cooperate for generation of endosomal tubules

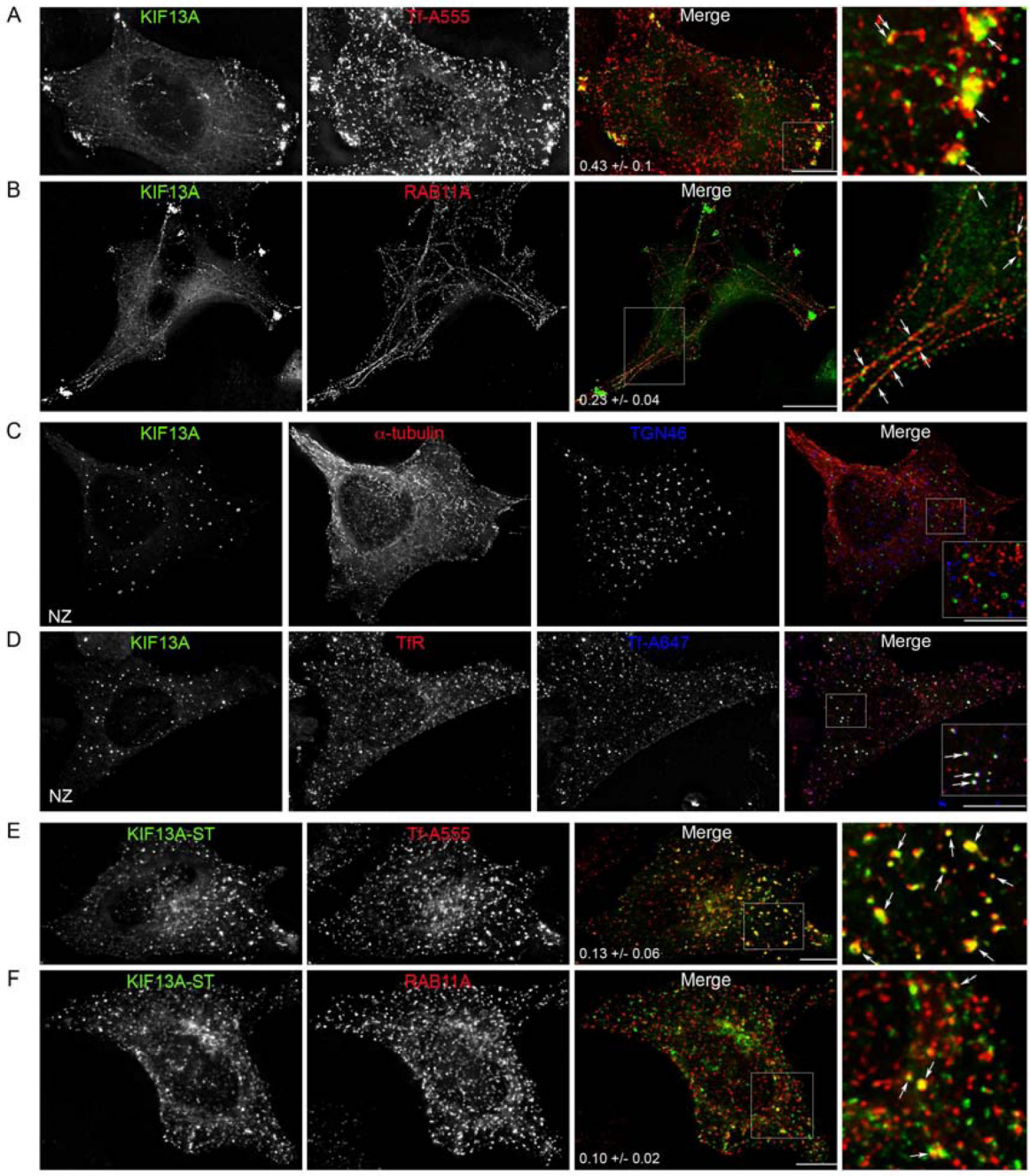

Figure 1. KIF13A localizes to recycling endosomes and controls their distributions in a microtubule-dependent manner

(**A–B**) IFM on KIF13A-expressing cells that internalized Tf-A555 (30 min) (**A**) before or after labeling for RAB11A (**B**). KIF13A co-distributes with RE (arrows) and generates RE tubules (**B**, arrows; and Movies 1–2). (**C–D**) IFM on KIF13A-expressing cells incubated with 10 μM nocodazole (NZ) and co-labeled for α–tubulin and TGN46 (**C**) or for TfR after Tf-A647 internalization (30 min) (**D**). NZ treatment disrupts the microtubule network and disperses TGN46 labeling (**C**), and prevents KIF13A-dependent RE tubulation (**C–D**, 1st panel) without affecting KIF13A endosomal localization (**D**, arrows). (**E–F**) IFM on KIF13A-ST-expressing cells that internalized Tf-A555 (30 min) (**E**) or after labeling for

RAB11A (**F**). KIF13A-ST co-distributes with RE (arrows) without generating tubules (arrows; and Movie 3). Bars, 10 μm. (See also Figures S1–S2–S3 and Movies 1–2–3).

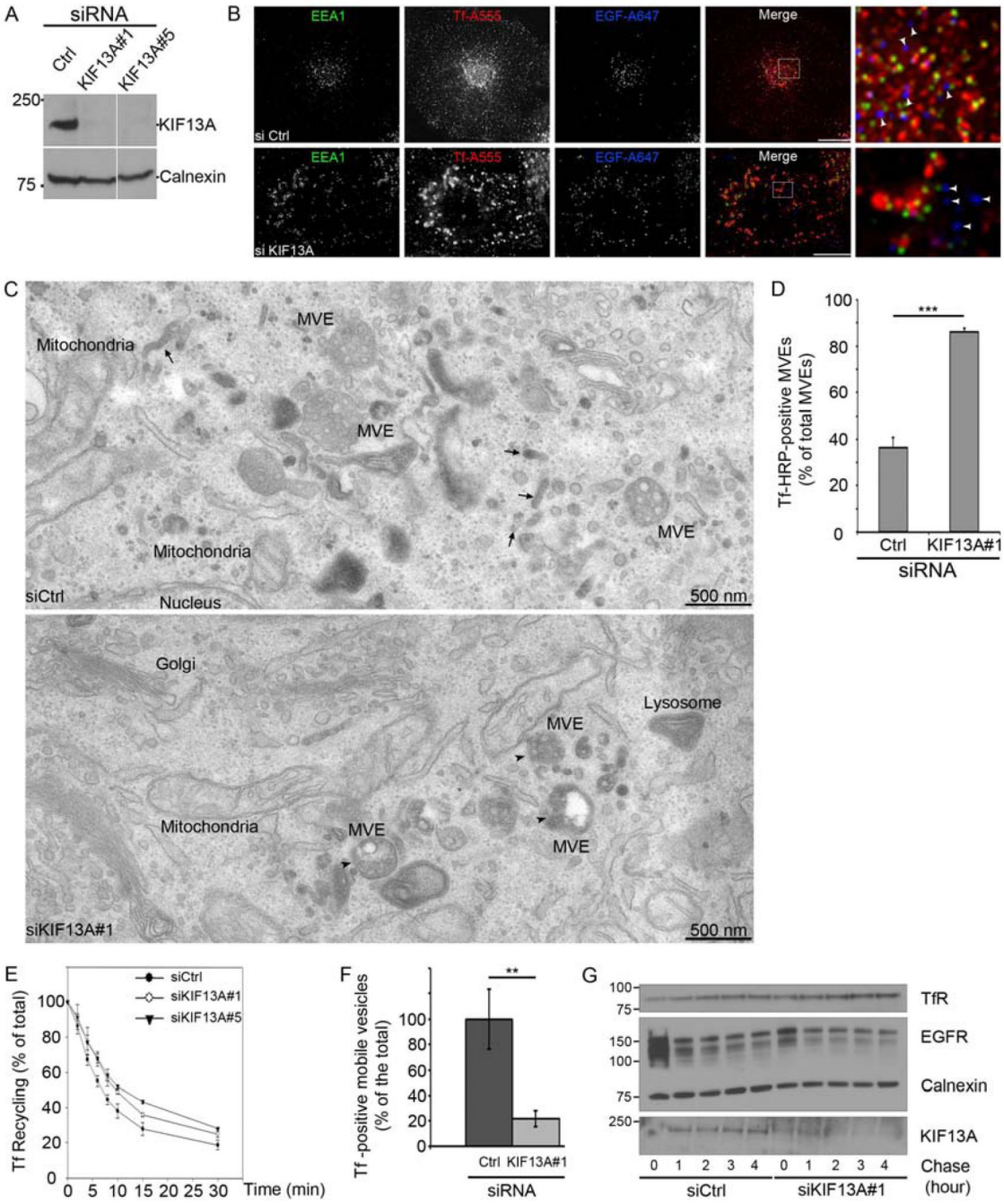

Figure 2. KIF13A controls the formation and function of recycling endosome tubules

(**A**) Western Blot (WB) of control (Ctrl)- or KIF13A-inactivated cell lysates (two different siRNAs -KIF13A#1 or #5-) probed for KIF13A or calnexin antibodies (loading control). (**B**) IFM on Ctrl- and KIF13A-inactivated cells pulsed with Tf-A555 and EGF-A647 (30 min), chased (30 min) and labeled for EEA1. EGF compartments were distinct from Tf- or EEA1-SE (arrowheads). (**C**) Conventional EM on Ctrl- or KIF13A-inactivated cells that internalized Tf-HRP and processed for DAB/H_2O_2 cytochemistry. Electron-dense Tf-HRP localized to tubulovesicular structures in Ctrl cells (arrows) while accumulated within MVEs in KIF13A-depleted cells (arrowheads). (**D**) Tf-HRP-positive MVEs (reported as a fraction

of total MVEs) increased up to 85±4 % in KIF13A-depleted cells (n=238) as compared to control (36±2 %; n=96). Data were presented as a mean ± SD. ***, p<0.001. (**E**) The recycling of Tf was measured in Ctrl- (black star) or KIF13A-siRNA-treated cells (KIF13A#1, white star; #5, black triangle). Intracellular Tf percentage was plotted according to the time of chase. Both siKIF13A inhibited 15% of the Tf recycling by 6 min of chase. Data are presented as the average of 3 independent experiments, normalized to control and presented as a mean ± SD. (**F**) Ctrl- and KIF13A-inactivated cells that internalized Tf-A555 were captured by TIRF microscopy. Mobile Tf-positive structures were quantified, normalized to their total number and decreased upon KIF13A inactivation as compared to Ctrl. Data are presented as a mean ± SD. **; p< 0.005. (**G**) Ctrl- and KIF13A-inactivated cells were processed as in **B**, chased for the indicated time, analyzed by WB probed for TfR, EGFR (positive control), Calnexin (loading control) or KIF13A (depletion control) antibodies. Data are from one experiment representative out of three. Molecular masses, kDa. Bars: IFM, 10μm; EM, 500 nm. (See also Figure S4).

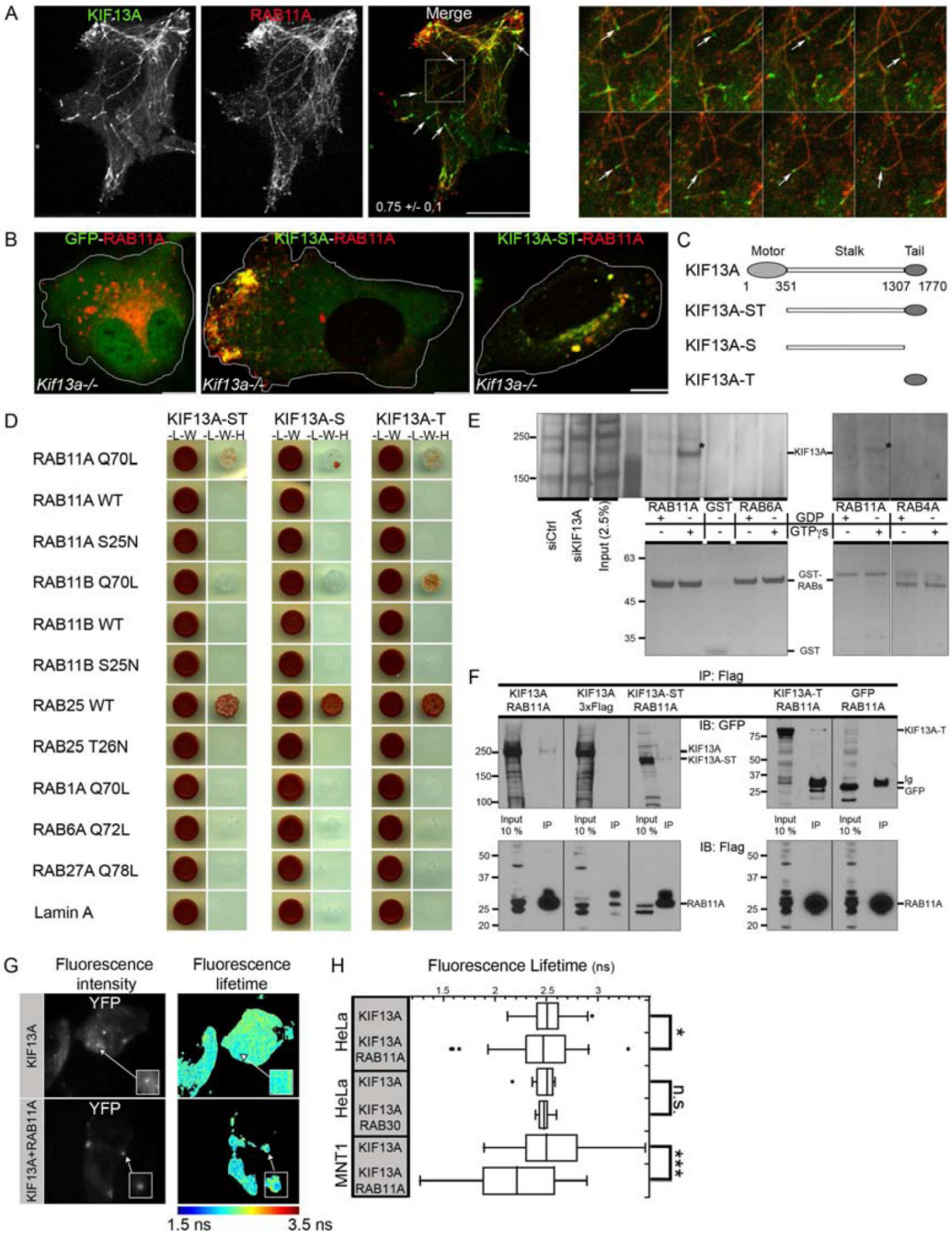

Figure 3. KIF13A associates dynamically and interacts with active RAB11

(**A**) Concomitant movements of KIF13A-YFP and mCherry-RAB11A were captured by spinning-disc microscopy. KIF13A induced an extensive tubulation and peripheral redistribution of RAB11A (see Movie 2). Magnified insets (of boxed area) of consecutive time-lapse images (image/6 sec) showed that KIF13A localized to the tip of RAB11A-positive tubule (arrows). (**B**) *Kif13a*$^{-/-}$ MEF cells were co-transfected for mCherry-RAB11A together with GFP, KIF13A-YFP or GFP-KIFF13A-ST. RAB11A localized to vesicles apposed to nuclei of GFP- or KIF13A-ST-cells, while KIF13A redistributed RAB11A towards the cell periphery (white contours). (**C**) Domain structure of KIF13A

revealed the motor domain (1–351), a Stalk region (352–1307) and a C-terminal Tail domain (1308–1770). (**D**) Y2H was performed to detect KIF13A/ RAB11 interactions. KIF13A Stalk and Tail interact with the GTPase-deficient (Q/L)-RAB11A, -RAB11B and wild-type RAB25. (**E**) Cell lysates incubated with GST, GST-RAB6A, -RAB4A or -RAB11A preloaded with GDP or GTPγs were analyzed by WB using KIF13A antibodies (top panel) or stained with coomassie blue (loading control; bottom panel). Lysates of Ctrl- and KIF13A-inactivated cells and experimental input showed KIF13A enrichment in RAB11A-pulled-down extracts. (**F**) Anti-Flag immunoprecipitations on lysates of cells co-expressing KIF13A-YFP, GFP-KIF13A-ST, GFP-KIF13A-T or GFP together with Flag-RAB11A or KIF13A-YFP with and empty Flag vector were analyzed by WB using GFP (upper panel) or Flag antibodies (lower panel). Inputs correspond to 10% of the whole cell lysates. (**G**) YFP fluorescence intensity (left) and FLIM (right) images of KIF13A-YFP-positive cells co-transfected (bottom) or not (top) with mCherry-RAB11A. The color-coding bar of FLIM images indicates YFP fluorescence lifetime value. (**H**) Fluorescence lifetime decreased in co-transfected cells indicating FRET between KIF13A and RAB11A in Hela (*; $p<0.05$) and MNT1 cells (***; $p<0.001$) as compared to control - no FRET was measured between KIF13A and RAB30 in HeLa cells. Molecular masses, kDa. Bars, 10 μm. (See also Movies 2 and 4).

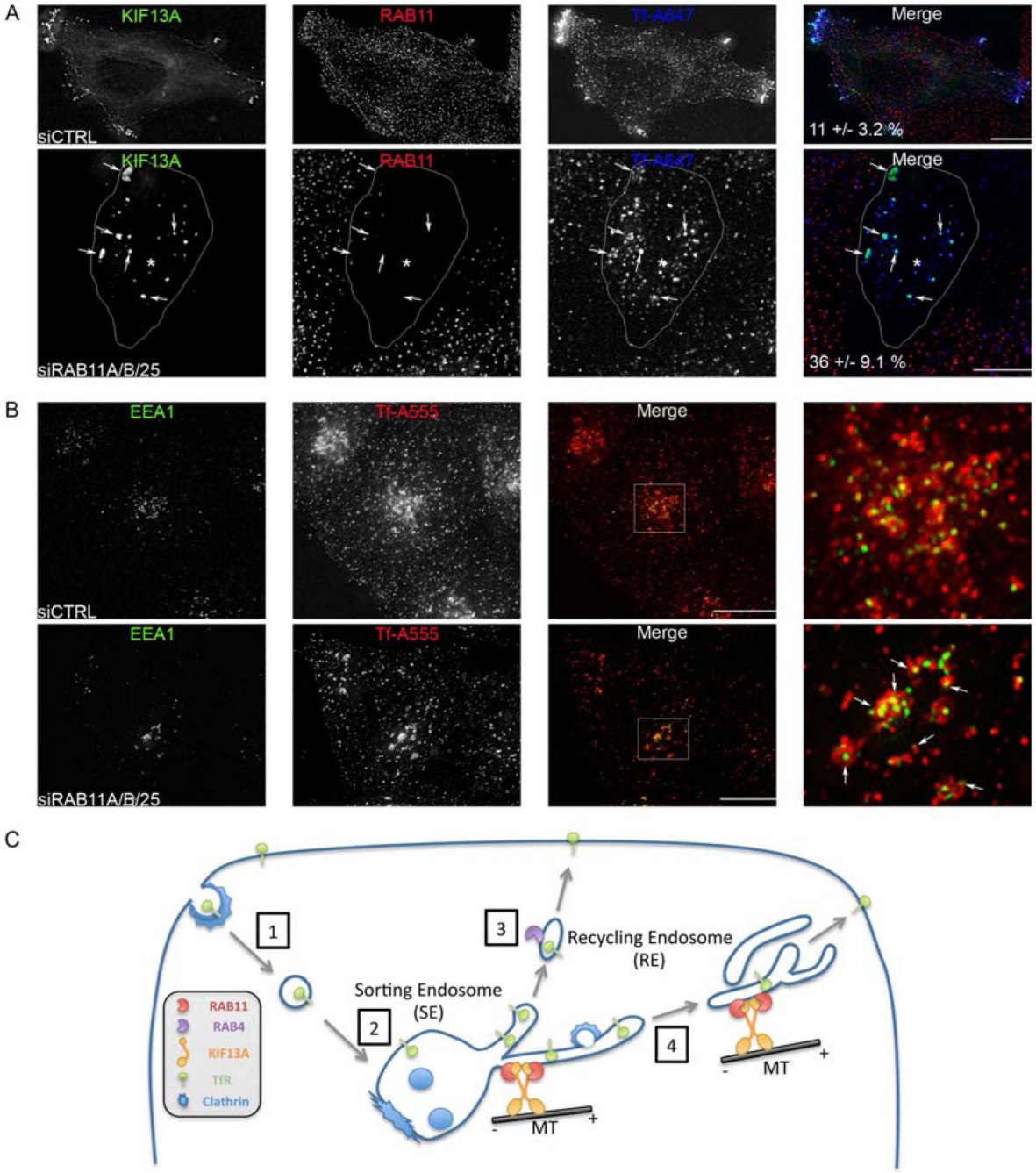

Figure 4. KIF13A and RAB11 cooperate to generate endosomal tubules

(**A–B**) Ctrl- and triple RAB11 (A/B/25)-depleted cells transfected (**A**) or not (**B**) with KIF13A were pulsed with Tf-A647 (30 min), chased (20 min), fixed and labeled for RAB11A (**A**) or EEA1 (**B**). RAB11-depleted cells (**A**, white star) accumulated either enlarged KIF13A- and Tf-positive endosomal compartments (arrows; $p<0.001$) or enlarged EEA1- and Tf-positive SE without KIF13A overexpression (**B**, arrows) as compared to control. (**C**) Proposed model for KIF13A function. The TfR bound to Tf is internalized via clathrin-coated pits (1) that uncoat and fuse with vacuolar sorting endosomes (SE) (2). TfR segregates rapidly within tubular domains for recycling to the plasma membrane by two

distinct routes: a fast RAB4-dependent pathway (3) or a slow RAB11-dependent route mediated by tubular transport intermediates (4). KIF13A functions at the SE and drives the generation, extension and peripheral transport of RAB11-dependent recycling endosome (RE) tubules in a microtubule- (MT) dependent manner. The formation of RE likely requires the interaction of KIF13A with RAB11 active form at specific SE subdomains, allowing the coordination between recycling of cargoes and proper maturation of SE. Bars, 10 μm.